Colloid Polym Sci (2003) 282: 21–31
DOI 10.1007/s00396-003-0897-y

ORIGINAL CONTRIBUTION

Susana Shimizu
Omar A. El Seoud

2-(Acylaminoethyl)trimethylammonium chloride surfactants: synthesis and properties of aqueous solutions

Received: 22 November 2002
Accepted: 4 March 2003
Published online: 24 May 2003
© Springer-Verlag 2003

S. Shimizu · O.A. El Seoud (✉)
Instituto de Química,
Universidade de São Paulo, C.P. 26077,
05513-970 São Paulo, SP, Brazil
E-mail: elseoud@iq.usp.br
Fax: +55-11-30913874

Abstract The title cationic surfactants have been synthesized by reaction of carboxylic acids with *N*,*N*-dimethylethylenediamine to give an intermediate amidoamine. The latter was quaternized with methyl iodide; the product was transformed into the corresponding chloride surfactant by ion-exchange on a macroporous resin. Adsorption and aggregation of these surfactants in H_2O have been studied by surface tension measurement. Additionally, solution conductivity, electromotive force (H_2O), and Fourier transform IR spectroscopy (D_2O) have been employed to investigate micelle formation. Increasing the length of *R* resulted in the following changes: an increase in the micelle aggregation number; a decrease in the minimum area per surfactant at the solution/air interface, the critical micelle concentration, and the degree of counterion dissociation. Gibbs free energies of adsorption at the solution/air interface and micelle formation in water were calculated and compared to those of alkyltrimethylammonium chlorides. The contribution to these free energies from surfactant methylene groups (in the hydrophobic tail) and the head group was calculated. The former are similar to those of other cationic surfactants. The corresponding free-energy contributions of head groups are smaller (i.e., more negative), indicating that the transfer of this group from bulk water to the interface (for adsorption) and/or to the micelle (aggregate formation) is more favorable. This is attributed to intermolecular hydrogen bonding of monomers at the interface, and/or in the aggregate, via the amide group, in agreement with our Fourier transform IR data. Our results are compatible with a micellar interface closer to the amide nitrogen than to the quaternary ammonium ion.

Keywords 2-(Acylaminoethyl)trimethylammonium chloride surfactants · Properties of cationic surfactants · Critical micelle concentration · Counterion dissociation · Aggregation number

Introduction

Understanding the relationship between the structure of surfactants and the properties of their aqueous solutions is relevant to important applications, inter alia, foaming, detergency, and emulsification. Examples include the dependence of electrolyte-induced changes insolution viscosity and rheology of surfactants on the nature of the counterion and the dependence of the number and the microstructure of phases in phase diagrams of nonionic surfactants on their hydrophile–lipophile balance [1, 2, 3]. In this regard, cationic surfactants offer a wealth of information because it is possible to vary the lengths of their hydrophobic tails, the nature of the counterions, and the volumes of their head groups. For example, in the series $C_{12}H_{25}N^+R_3Br^-$, increasing the length of R from methyl to *n*-butyl decreased the Gibbs free energy of micellization [4], and caused a gradual dehydration of the interfacial region [5]. For anionic surfactants, the corresponding structural change involves studying head groups of different chemical nature, for example, carboxylate, sulfonate, or phosphate.

Available information on cationic surfactants that carry the amide head group is focused on the synthesis and the biological activity of commercial products, i.e., where the tail is a mixture of hydrocarbon groups [6, 7]. This prompted us to start a systematic study on this group of surfactants, in order to understand the relationship between the previously mentioned structural variables and the properties of their aqueous solutions.

The series that we previously studied include 2-aminoglucose based anionic and cationic surfactants [8], and benzyl-(2-acylaminoethyl)dimethylammonium chlorides, $RCONH(CH_2)_2N^+(CH_3)_2CH_2C_6H_5Cl^-$, where $RCO = C_{10}$–C_{16}, respectively [9]. Our results indicate that the interfacial amide group favors adsorption and micellization, owing to hydrogen bonding between surfactant monomers, akin to those formed by *N*-alkylamides, and polypeptides [10, 11]. There is also some information, for example, on the phase behavior of other amide-group-carrying surfactants [12].

We report here on the synthesis of the following series of surfactants: $RCONH(CH_2)_2N^+(CH_3)_3Cl^-$, where $RCO = C_{10}$, $C_{10}A\mathrm{Me}_3\mathrm{Cl}$; C_{12}, $C_{12}A\mathrm{Me}_3\mathrm{Cl}$; C_{14}, $C_{14}A\mathrm{Me}_3\mathrm{Cl}$; and C_{16}, $C_{16}A\mathrm{Me}_3\mathrm{Cl}$, where A and Me_3 stand for $–NH(CH_2)_2–$ and the trimethylammonium group, respectively. Solution conductivity, surface tension, electromotive force (EMF), and Fourier transform IR (FTIR) data were employed for calculation of the following micellar properties: the critical micelle concentration (cmc), the degree of micelle counterion dissociation, α_{mic}, the aggregation number, N_{agg}, as well as the Gibbs free energies of adsorption at the solution/air interface, $\Delta G^0_{\mathrm{ads}}$, and/or of micellization, $\Delta G^0_{\mathrm{mic}}$. Contributions of the structural segments to the latter two quantities were also calculated. For the present series, $\Delta G^0_{\mathrm{ads}}$ and $\Delta G^0_{\mathrm{mic}}$ are more favorable than those of other cationic surfactants, for example, alkyltrimethylammonium chlorides, $R'\mathrm{Me}_3\mathrm{Cl}$, where R' is decyl to hexadecyl. This is attributed to the previously mentioned hydrogen bonding between adsorbed and/or aggregated surfactant monomers. This conclusion is supported by an FTIR study in which we investigated the dependence of the frequency of amide I band on the surfactant concentration. Our results indicate that the micellar interface lies behind the quaternary ammonium ion, close to the amide group.

Experimental

Materials

The solvents and reagents were purchased from Aldrich or Merck. Methyl iodide and *N*,*N*-dimethylethylenediamine were purified by fractional distillation (the latter from CaH_2). Commercial "anhydrous" ethanol (Penta Química, São Paulo) was further dried by azeotropic distillation. Other reagents were employed as received.

Apparatus

Melting points were determined with an IA 6304 apparatus (Electrothermal, London, UK). Gas chromatographic analysis was carried out with a model GC 17A-2 gas chromatograph (Shimadzu, Kyoto, Japan), as reported elsewhere [9]. Microanalyses were carried out at the microanalysis laboratory of this institute. FTIR spectra were recorded with a Bruker Vector 22 spectrophotometer. ^1H and ^{13}C NMR spectra were recorded with Varian Innova-300 or Bruker DRX-500 spectrometers.

Synthesis

The synthetic route employed is depicted in Scheme 1, where RCO_2H refers to decanoic, dodecanoic, tetradecanoic, and hexadecanoic acid, respectively, and Res-Cl refers to a macroporous ion-exchange resin in the chloride form.

$RCONH(CH_2)_2N(CH_3)_2$

Amidoamines, **1a**–**1d**, $RCONH(CH_2)_2N(CH_3)_2$ were prepared as described elsewhere by reacting chromatographically pure carboxylic acids with *N*, *N*-dimethylethylenediamine in toluene, followed by removal of water produced by azeotropic distillation. The physical properties and characterization of these compounds are reported elsewhere [9].

Scheme 1

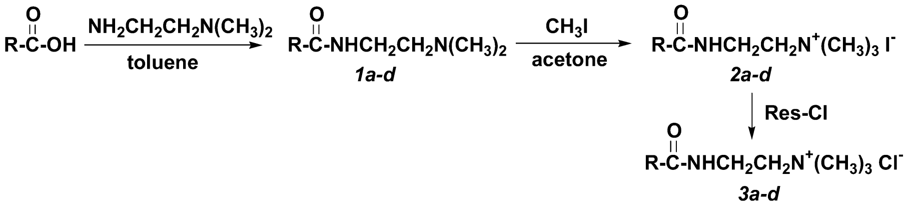

*R*CONH(CH$_2$)$_2$N$^+$(CH$_3$)$_3$I$^-$

The following reaction was carried out under dry, oxygen-free nitrogen, in the absence of light. A mixture of 0.1 mol compound **1** and 7.16 ml (0.115 mol) methyl iodide in 100 ml of anhydrous acetone was refluxed for 6 h. The solvent and unreacted methyl iodide were removed, the product was recrystallized from a mixture of anhydrous acetone/ethanol, then dried under reduced pressure, over P_4O_{10}.

The following results were obtained, see structure later, where *n* is the total number of carbon atoms of the precursor acid. In what follows, all IR frequencies are given in reciprocal centimeters, NMR chemical shifts, δ, and coupling constants, *J*, are given in parts per million, and hertz, respectively.

$$\underset{1}{\mathrm{CH_3}} - \underset{2}{\mathrm{CH_2}} - \underset{3}{\mathrm{CH_2}} - \underset{4}{(\mathrm{CH_2})_{n-7}} - \underset{5}{\mathrm{CH_2}} - \underset{6}{\mathrm{CH_2}} - \underset{7}{\mathrm{CH_2}} - \mathrm{CO} - \mathrm{NH}$$
$$- \underset{8}{\mathrm{CH_2}} - \underset{9}{\mathrm{CH_2}} - \mathrm{N^+}\, \underset{10}{(\mathrm{CH_3})_3}\, \mathrm{I^-}$$

Compound **2a**

White solid, yield, 78%, m.p. = 122–124 °C, Anal. Calcd for $C_{15}H_{33}IN_2O$: C, 46.88; H, 8.65; N, 7.29. Found: C, 46.99; H, 8.49; N, 7.31. IV (KBr) 3386 ($\nu_{N\text{–}H}$, secondary amide), 1659 (amide I band, due to ν_{CO}, coupled with an out-of-phase $\nu_{C\text{–}N}$ and an in-plane N–H bending mode), 1526 (amide II band, due to $\nu_{(O)C\text{–}N}$ coupled with in-plane N–H bending mode). ^{1}H NMR (CDCl$_3$): 0.88 (t, 3H, H1, $J_{1\text{–}2} = 6.7$), 1.26 (broad singlet, 12H, H2–5), 1.61 (quintet, 2H, H6, $J_{5\text{–}6}$ and $J_{6\text{–}7} = 7.4$), 2.28 (t, 2H, H7), 3.87 (multiplet, 2H, H8), 3.81 (t, 2H, H9, $J_{8\text{–}9} =$ 5.22), 3.45 (s, 6H, H10), 7.64 (t, 1H, NH, $J_{H7\text{-}NH} =$ 5.6).

Compounds **2b–2d**

The spectroscopic data of **2b**–**2d** were similar to those of compound **2a**, within the following limits: IR (± 2 cm^{-1}), ^{1}H NMR (0 to ± 0.02 ppm).

2b: White solid, yield, 84%, m.p. = 125–127 °C, Anal. Calcd for $C_{17}H_{37}IN_2O$: C, 49.51; H, 9.04; N, 6.79. Found: C, 49.49; H, 8.37; N, 6.95. **2c**: White solid, yield, 95%, m.p. = 126–128 °C, Anal. Calcd for $C_{19}H_{41}IN_2O$: C, 51.81; H, 9.38; N, 6.36. Found: C, 51.82; H, 8.76; N, 6.51. **2d**: White solid, yield, 92%, m.p. = 128–130 °C, Anal. Calcd for $C_{21}H_{45}IN_2O$: C, 53.84; H, 9.68; N, 5.98. Found: C, 53.87; H, 8.91; N, 6.24.

*R*CONH(CH$_2$)$_2$N$^+$(CH$_3$)$_3$Cl$^-$

Each of the iodides **2a**–**2d** was dissolved in absolute ethanol and passed through a column of Amberlyst A-27 macroporous anion-exchange resin. The later was in the chloride form, and was previously equilibrated with ethanol. The eluted solution was dried under reduced pressure, and the white residue was recrystallized from a mixture of anhydrous acetone/ethanol. The surfactant yields were 80 ± 5%, all surfactants were white, hygroscopic solids, and were analyzed as (nonhygroscopic) perchlorates.

Surfactant **3a**

C$_{10}$*A*Me$_3$Cl: Anal. Calcd. for $C_{15}H_{33}N_2ClO_5$: C, 50.48; H, 9.32; N, 7.85. Found: C, 50.79; H, 9.05; N, 7.90. ^{1}H NMR (CDCl$_3$), proton numbering as for **2a**: 0.88 (t, 3H, H1, $J_{1\text{–}2} = 6.6$), 1.25 (broad singlet, 12H, H2–H5), 1.59 (quintet, 2H, H6, $J_{5\text{–}6}$ and $J_{6\text{–}7} = 7.5$), 2.26 (t, 2H, H7), 3.78 (multiplet, 4H, H8 and H9, 3.43 (s, 6H, H10), 8.60 (apparent triplet, 1H, NH). ^{13}C NMR (CDCl$_3$): 14.01 (C1), 22.57 (C2), 31.78 (C3), 29.21–29.41, C4–C5 (four lines), 25.45 (C6), 34.21 (C7), 36.20 (C8), 65.40 (C9), 53.95 (C10), 174.74 (CO).

Surfactant **3b**

C$_{12}$*A*Me$_3$Cl: Anal. Calcd. for $C_{17}H_{37}N_2ClO_5$: C, 53.04; H, 9.69; N, 7.28. Found: C, 53.07; H, 9.06; N, 7.27. The spectroscopic data of **3b**–**3d** were similar to those of compound **3a**, within the following limits: ^{1}H NMR (0 to ± 0.05 ppm) and ^{13}C NMR (± 0.16 ppm). The spectral region for C4–C5 showed six lines.

Surfactant **3c**

C$_{14}$*A*Me$_3$Cl: Anal. Calcd. for $C_{19}H_{41}N_2ClO_5$: C, 55.26; H, 10.01; N, 6.78. Found: C, 55.48; H, 9.24; N, 6.82. The spectral region for C4–C5 showed seven lines.

Surfactant **3d**

C$_{16}$*A*Me$_3$Cl: Anal. Calcd. for $C_{21}H_{45}N_2ClO_5$: C, 57.19; H, 10.28; N, 6.35. Found: C, 57.09; H, 9.56; N, 6.28. The spectral region for C4–C5 showed eight lines.

Sodium 2-decanoyloxyethane sulfonate (sodium decanoylisethionate)

$$\underset{1}{\mathrm{CH_3}} - \underset{2}{\mathrm{CH_2}} - \underset{3}{\mathrm{CH_2}} - \underset{4}{(\mathrm{CH_2})_4} - \underset{5}{\mathrm{CH_2}} - \underset{6}{\mathrm{CH_2}} - \underset{7}{\mathrm{CH_2}} - \mathrm{CO} - \mathrm{O}$$
$$- \underset{8}{\mathrm{CH_2}} - \underset{9}{\mathrm{CH_2}} - \mathrm{SO_3^-Na^+}$$

Decanoyl chloride was prepared by mixing 17.85 g (0.10 mol) decanoic acid with 8.9 ml (0.12 mol) thionyl chloride, followed by refluxing for 1 h. The acyl chloride (92% yield) was purified by fractional distillation, 100–102 °C/6 mmHg.

Commercial sodium 2-ethanesulfonate (Oxiteno, São Paulo), 4.44 g (0.03 mol), was suspended in 30 ml dry dimethoxyethane. Pyridine, 4.8 ml (0.06 mol), was added under vigorous agitation, followed by 5.9 ml (0.03 mol) decanoyl chloride. The mixture was refluxed for 9 h, the solvent was evaporated, the solid product was suspended three times in chloroform, filtered, and was crystallized from anhydrous acetone.

White solid, yield 25%, Anal. Calcd for $C_{12}H_{23}NaO_5S$: C, 47.67; H, 7.67. Found: C, 45.93; H, 7.01.

^{1}H NMR (DMSO-d_6): 0.85 (t, 3H, H1, $J_{1\text{–}2} = 6.6$); 1.23 (broad singlet, 12H, H2–H5); 1.49 (quintet, 2H, H6, $J_{6\text{–}7}$ and $J_{7\text{–}8} = 6.7$); 2.25 (t, 2H, H7); 2.75 (t, 2H, H9, $J_{8\text{–}9}$); 4.19 (t, 2H, H8). ^{13}C NMR (DMSO-d_6): 13.83 (C1); 21.97 (C2); 24.30 (C6); 29.21–28.33 (C4–C5, four lines); 31.15 (C3); 33.38 (C7); 49.95 (C9); 60.59 (C8); 54.03 (C9); 174.75 (CO).

Measurement of surface-active properties

Glass double-distilled, deionized water was used throughout. In order to avoid any interference from traces of heavy metal ions [13], all glassware was soaked in 0.001 M ethylenediaminetetraacetate solution and thoroughly washed with water.

Surface tension

The solution surface tension was measured at 25 °C with a Lauda TE1C digital ring tensiometer, equipped with a thermostated solution compartment, and controlled with a home-developed software package. The standard deviation among four successive readings was less than 0.10 mN m^{-1}.

Solution conductivity

Conductivity measurements were recorded at 25 °C with a personal computer interfaced Fisher model Accumet 50 pH meter/conductimeter, provided with a Digimed model DM-C1 microconductivity cell (Digimed, São Paulo) and Schott model Titronic T200 programmed burette. A home-developed software package was used both for programmed dilution of the concentrated surfactant solution and acquisition of conductance data.

Electromotive force measurements

The previously mentioned pH meter/conductimeter was employed for measuring the EMF, at 25 °C. A Corning double-junction Ag/AgCl reference electrode, and IS-146Cl chloride-selective electrode (Lazar Research Laboratories, Los Angeles, USA) were employed.

FTIR measurements

The cmc of $C_{10}A\text{Me}_3\text{Cl}$ in D_2O was determined by FTIR spectroscopy, by employing the previously mentioned spectrophotometer and a 0.015-mm path length ClearTran cell (Wilmad Glass, NJ). The spectrophotometer sample compartment was flushed with dry nitrogen, thermostated at 25 °C. The amide I band was measured (1-cm^{-1} resolution) as function of surfactant concentration. $\nu_{C=O}$ of duplicate runs agreed within this resolution limit. The background spectrum of pure D_2O was subtracted from the spectrum of the sample (Bruker Opus-NT, version 3.0). The same procedure was employed for sodium isethionate.

Results and discussion

Synthesis

Amidoamines were synthesized by reacting *N*,*N*-dimethylethylenediamine with precursor carboxylic acid, rather than its acyl chloride (plus tertiary amine catalyst) [6, 7], for the following reason: the reaction product, $R\text{CONH}(\text{CH}_2)_2\text{N}(\text{CH}_3)_2$, is also a tertiary amine and will, in principle, compete for the HCl produced to form a (difficult-to-remove) cationic surfactant impurity. The completeness of this condensation reaction is indicated by the absence of IR absorption at around 1725 cm^{-1}, due to unreacted acid. Use of chromatographically pure fatty acids and exclusion of oxygen during the synthesis (to avoid formation of amine-oxide impurities) are crucial in order to obtain surface-active pure surfactants.

Properties of aqueous solution

The following discussion is organized in terms of the sequence of events that occur in the system, that is, adsorption of the surfactant at the solution/air interface, followed by its aggregation. Data for the series studied are compared with those of alkyltrimethylammonium chlorides, $R'\text{Me}_3\text{Cl}$, where R' is decyl to hexadecyl. In the last section of the Results and discussion we compare $RA\text{Me}_3\text{Cl}$ with the corresponding benzyl-(2-acylaminoethyl)dimethylammonium chlorides, $RA\text{BzMe}_2\text{Cl}$, i.e., we address effects of substitution of a benzyl group for one of the trimethylammonium groups on solution properties. Details of the calculations of all quantities discussed in this work are given in the Appendix, vide infra.

Adsorption at solution/air interface

The solution surface tension at the cmc, γ_{cmc}, the surfactant concentration required to decrease the surface tension of water by 20 mN m^{-1}, C_{20}, the minimum area per surfactant molecule at the solution/air interface, A_{min}, and the Gibbs free energy of adsorption, ΔG^0_{ads}, are listed in Table 1. In comparing the $RA\text{Me}_3\text{Cl}$ and $R'\text{Me}_3\text{Cl}$ data, allowance should be made for the fact that the surface tension measurements were carried out in distilled water, and synthetic river (hard) water, respectively [15]. In the latter case, the high ionic strength and common-ion effect (with surfactant counterion) enhance surfactant adsorption at the solution/air interface [2], this explains, for example, the result that $\left|\Delta G^0_{\text{ads}}\right|_{R'\text{Me}_3\text{Cl}} > \left|\Delta G^0_{\text{ads}}\right|_{RA\text{Me}_3\text{Cl}}$, see Table 1. The effectiveness of adsorption (γ_{cmc}), and the efficiency of adsorption (C_{20}) are important for comparing the performance of surfactants in, for example, wetting and emulsification. In agreement with previous results [2],

Table 1 Adsorption properties of the surfactants studied compared with other cationic surfactants, at 25 °C. γ_{cmc}, (C_{20}), A_{min}, and ΔG^0_{ads} refer to the solution surface tension at the critical micelle concentration (*cmc*), the surfactant concentration required to decrease the surface tension of water by 20 mN m^{-1}, the area per surfactant molecule at the interface, and the Gibbs free energy of adsorption, respectively

Surfactant	γ_{cmc} (mN m^{-1})	$10^3 C_{20}$ (mol L^{-1})	A_{min} (nm^2)	ΔG^0_{ads} (kJ mol^{-1})
$C_{10}A\text{Me}_3\text{Cl}$	39.0	12.3	0.78	−30.5
$C_{12}A\text{Me}_3\text{Cl}$	42.0	3.78	0.74	−32.9
$C_{14}A\text{Me}_3\text{Cl}$	43.4	1.57	0.66	−34.0
$C_{16}A\text{Me}_3\text{Cl}$	43.4	0.34	0.60	−37.1
$C_{10}\text{Me}_3\text{Cl}$[a]	42.0	6.6	0.87	−32.9
$C_{12}\text{Me}_3\text{Cl}$[a]	41.8	1.6	0.62	−33.3
$C_{14}\text{Me}_3\text{Cl}$[a]	40.0	0.28	0.53	−36.6
$C_{16}\text{Me}_3\text{Cl}$[a]	37.6	0.04	0.49	−40.8
$C_{10}A\text{BzMe}_2\text{Cl}$[b]	39.0	5.9	0.87	−33.3
$C_{12}A\text{BzMe}_2\text{Cl}$[b]	39.6	1.6	0.82	−35.9
$C_{14}A\text{BzMe}_2\text{Cl}$[b]	39.9	0.40	0.79	−38.9
$C_{16}A\text{BzMe}_2\text{Cl}$[b]	42.2	0.11	0.73	−41.3

[a] Data from Ref. [15], measurements carried out in synthetic river (hard) water

[b] Data from Ref. [9]

as a function of increasing length of R or R', the effectiveness shows little variation, whereas the efficiency increases. There is little dependence on the structure of the head group.

All surfactants listed in Table 1 show that $A_{\min}$ decreases as a function of increasing the length of R, or R', owing to concomitant closer packing of monomers in the micelle [1, 2, 3]. It is known that surfactant molecules lie titled to the interface. Comparison of $A_{\min}$ with the cross-section area of the head group (whose conformation was minimized by the PM3 semiempirical method) indicated that a part of the group $\text{–CONH–(CH}_2)_2\text{–N}^+(\text{CH}_3)_3$ must lie at the solution/air interface. For example, the cross-section areas of $\text{–N}^+(\text{CH}_3)_3$ and $\text{–CONH–(CH}_2)_2\text{–N}^+(\text{CH}_3)_3$ are 0.45 and 1.2 nm^2, respectively. This calculation and the fact that $A_{\min}$ is larger for RAMe$_3$Cl than for the corresponding R'Me$_3$Cl show that the hydrated head group of the former is rather large. One possibility is that the micellar interface lies behind the $\text{–N}^+(\text{CH}_3)_3$ group, as discussed later.

The Gibbs free energy of adsorption, ΔG^0_{ads}, is calculated from C_{20} and $A_{\min}$. It contains contributions from the transfer of surfactant segments from bulk water to the interface. These are due to the terminal CH$_3$ group of the hydrophobic chain, $\Delta G^0_{\text{CH}_3}$, the methylene groups of the alkyl chain, $(N_{\text{CH}_2}\Delta G^0_{\text{CH}_2})$, where $N = 8$, 10, 12, and 14, respectively, and the head group, $\Delta G^0_{\text{head group}}$, as given by [2]

$$\Delta G^0_{\text{ads}} = \Delta G^0_{\text{head group}} + \Delta G^0_{\text{CH}_3} + N_{\text{CH}_2}\Delta G^0_{\text{CH}_2}. \qquad (1)$$

Equation (1) predicts a linear correlation between ΔG^0_{ads} and N_{CH_2}, where the intercept includes a contribution from the terminal methyl plus the head group. Since $\Delta G^0_{\text{CH}_3}$ is independent of the chain length of the surfactant, its contribution is constant in a homologous series. That is, the intercept essentially reflects the effect of transfer of the head group from bulk solution to the solution/air interface [14]. Application of Eq. (1) to the data of RAMe$_3$Cl gave a straight line (correlation coefficient $r = 0.9856$). The present study and previous ones on R'Me$_3$Cl [15, 16] gave the following results, respectively: −1.04 and −1.35 kJ mol^{-1} $(\Delta G^0_{\text{CH}_2})$; −22.2 and −19.7 kJ mol^{-1} $(\Delta G^0_{\text{head group}} + \Delta G^0_{\text{CH}_3})$. For the latter series, a better correlation is obtained if the point for C$_{10}$Me$_3$Cl is deleted (r increases from 0.9515 to 0.9976), giving −1.88 and −12.5 kJ mol^{-1}, for $\Delta G^0_{\text{CH}_2}$ and $(\Delta G^0_{\text{head group}} + \Delta G^0_{\text{CH}_3})$, respectively.

The similarity of $\Delta G^0_{\text{CH}_2}$ for RAMe$_3$Cl and R'Me$_3$Cl is expected because the transfer of a CH$_2$ group in the hydrophobic tail from the bulk phase to the interface should be independent of its hydrophilic moiety. The reason for the more favorable free energy of transfer of the head group of the former surfactant series will be discussed later.

Aggregation: cmc, degree of micelle dissociation, thermodynamic parameters of micellization, and aggregation numbers

Representative plots of solution conductance and surface tension as a function of surfactant concentration are shown in Fig. 1. The corresponding plots of the surfactant free counterion, [Cl$^-$]$_{\text{free}}$, and the IR frequency of the amide I band versus surfactant concentration are shown in Fig. 2. Each of the first three graphs consists of two straight lines intersecting at the cmc. There are two breaks in Fig. 2b, the first one at the cmc.

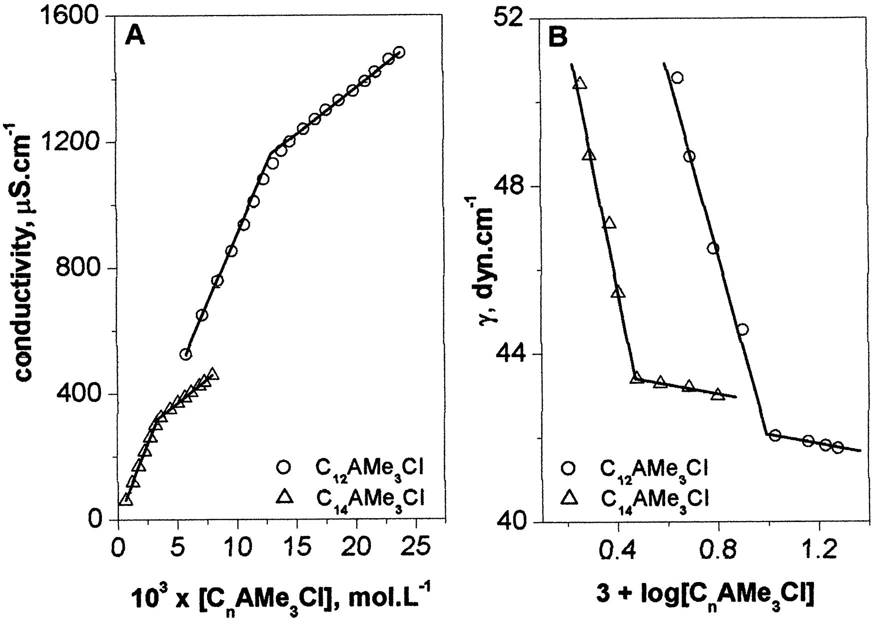

Fig. 1 Dependence of solution conductance **A** and surface tension **B** on surfactant concentration, at 25 °C

These values are listed in Table 2, along with literature data for the corresponding $R'Me_3Cl$.

Regarding these results, the following are relevant:

1. The EMF experiment was employed to calculate three micellar properties, namely, cmc, α_{mic}, and N_{agg}. The last two require measurements up to about 60 mc. The high solution viscosity precluded carrying out the experiment with $C_{10}AMe_3Cl$.

2. Conductance measurements were employed to obtain α_{mic} since data are available for all the surfactants studied. Calculation of α_{mic} may be carried out simply by dividing the slopes of the straight lines above and below the cmc. Frahm's method [17] is a useful approximation when N_{agg} is not available; it results in α_{mic} higher than that calculated by Evans' method, because the conductivity of the micelle (a "macroion") is

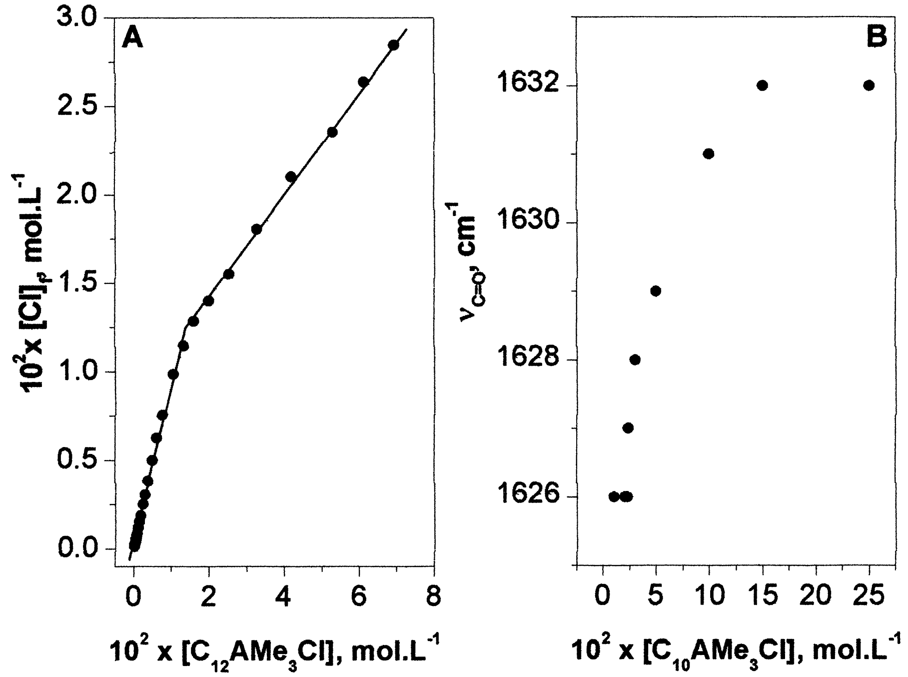

Fig. 2 Dependence of the concentration of the free counter-ion, $[Cl^-]_{free}$ **A** and $\nu_{C=O}$ of amide I band **B** on $C_{12}AMe_3Cl$ and $C_{10}AMe_3Cl$, respectively, at 25 °C. In **A**, the *points* are experimental data and the *line* was calculated as given in the Appendix

Table 2 Relationship between surfactant structure and cmc degree of micelle dissociation, α_{mic}, micelle aggregation number, N_{agg}, and Gibbs free energy of micelle formation, ΔG^0_{mic}, at 25 °C. All cmc values are in moles per liter and should be multiplied by 10^{-3}

Surfactant	cmc, surface tension	cmc, conductance	cmc, electromotive force	cmc/C_{20}	α_{mic}, conductance[a,b]	N_{agg}[c]		ΔG^0_{mic} kJ mol^{-1})[d]
						EMF	Calculated	
$C_{10}AMe_3Cl$	41.6	46.0	–[e]	3.74	0.37 (0.39)	–[e]	43	−28.6 (−28.2)
$C_{12}AMe_3Cl$	9.62	13.0	12.7	3.44	0.25 (0.34)	68	61	−36.3 (−34.4)
$C_{14}AMe_3Cl$	3.14	3.40	3.60	2.17	0.21 (0.33)	80	82	−43.0 (−40.1)
$C_{16}AMe_3Cl$	0.64	0.86	0.95	2.53	0.20 (0.35)	117	107	−49.4 (−45.4)
$C_{12}Me_3Cl$[f]		18		11	(0.42)			
$C_{14}Me_3Cl$[g]		3.4		12	(0.40)			
$C_{16}Me_3Cl$[f]		1.0		25	(0.38)			
$C_{10}ABzMe_2Cl$[g]	25	24.0	–[e]	4.07	0.28 (0.35)			−32.8 (−31.4)
$C_{12}ABzMe_2Cl$[g]	5.8	5.9	5.8	3.69	0.23 (0.35)	58	61	−40.1 (−37.3)
$C_{14}ABzMe_2Cl$[g]	1.3	1.5	1.5	3.75	0.22 (0.38)	84	82	−46.3 (−42.2)
$C_{16}ABzMe_2Cl$[g]	0.27	0.40	0.39	3.64	0.19 (0.38)	110	107	−53.0 (−47.5)

[a] α_{mic} was calculated by the method of Evans. The figures in *parentheses* refer to α_{mic}calculated by Frahm's method

[b] α_{mic} from electromotive force measurements was 0.24, 0.21, and 0.21 for $C_{12}AMe_3Cl$, $C_{14}AMe_3Cl$, and $C_{16}AMe_3Cl$, respectively

[c] Calculated from electromotive force measurements, or from the volumes of monomer and micelle, see the Appendix for details

[d] The figures in *parentheses* refer to free energies of micellization based on α_{mic} calculated by Frahm's method

[e] High solution viscosity precluded performing this experiment

[f] Results from Refs. [15, 20]

[g] Results from Ref. [9]

not taken into account [18]. The use of the Evans equation requires knowledge of N_{agg}; this was calculated from volumes of the monomer and micelle, respectively. The micellar interface may be located either at the amide group or at the quaternary ammonium ion of RCO–NH(CH$_2$CH$_2$)N$^+$(CH$_3$)$_3$Cl$^-$. Both assumptions were considered; the former N_{agg} were employed since the latter ones (72, 96, 122, and 152 for RCO= C_{10}, C_{12}, C_{14}, and C_{16}, respectively) were considered too high. We also employed our EMF data to calculate N_{agg}. As shown in the appropriate column of Table 2, there is excellent agreement between theoretically calculated and experimental aggregation numbers; this corroborates our view of the location of the interface;

3. The Gibbs free energy of micelle formation, ΔG^0_{mic}, is obtained from the cmc and α_{mic}, as given in the Appendix. For comparison with literature data, we carried out the calculations by using α_{mic} obtained by both methods (Table 2). Equation (2) for ΔG^0_{mic} is written analogously to Eq. (1) [2]:

$$\Delta G^0_{mic} = \Delta G^0_{head\ group} + \Delta G^0_{CH_3} + N_{CH_2}\Delta G^0_{CH_2}, \tag{2}$$

where the terms $\Delta G^0_{head\ group}$, $\Delta G^0_{CH_3}$, and $\Delta G^0_{CH_2}$ refer to contributions to ΔG^0_{mic} of the surfactant moieties, as discussed earlier for adsorption. Application of Eq. (2) to RAMe$_3$Cl gave an excellent straight line ($r = 0.9995$). The following results are for RAMe$_3$Cl and R'Me$_3$Cl [19, 20], respectively, and are based on α_{mic} calculated by Frahm's method: $\Delta G^0_{CH_2} = 2.9$ and -3.1 kJ mol^{-1}, and $(\Delta G^0_{head\ group} + \Delta G^0_{CH_3}) = -5.9$ and 2.4 kJ mol^{-1}. Again, whereas $\Delta G^0_{CH_2}$ is similar for the two surfactant series, the free energy of transfer of the head group of RAMe$_3$Cl from bulk solution to the micelle is more favorable than that of R'Me$_3$Cl. $\Delta G^0_{CH_2}$ and $(\Delta G^0_{head\ group} + \Delta G^0_{CH_3})$ based on α_{mic}, calculated by the Evans equation were found to be -3.5 and -0.86 kJ mol^{-1} ($r = 0.9991$), respectively.

4. The agreement between the cmc and α_{mic} calculated from data of four different techniques is satisfying, considering that the IR experiment was carried out in D$_2$O. This is one of the few studies in which IR spectroscopy has been used to determine the cmc of surfactants [21, 22], although IR and Raman spectroscopy have been fruitfully employed to study interactions (including hydrogen bonding) within organized assemblies [23, 24].

5. The concentration of the free counterion, [Cl$^-$]$_{free}$, and free surfactant cation, [S^+]$_{free}$, can be calculated from EMF data; a typical example is shown in Fig. 3 for C$_{14}$AMe$_3$Cl. Above the cmc, [Cl$^-$]$_{free}$ increases, [C$_{14}A$Me$_3{}^+$]$_{free}$ decreases, whereas the mean ionic molarity of the surfactant, i.e., ([Cl$^-$]$_{free}$×[C$_{14}A$Me$_3{}^+$]$_{free}$)$^{0.5}$ increases slowly, in agreement with the mass-action model for micelle formation, as discussed elsewhere [25].

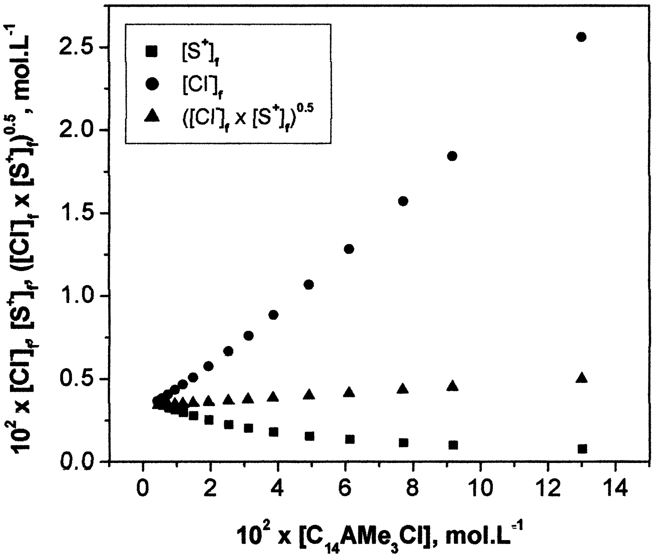

Fig. 3 Dependence of concentrations of the surfactant free counterion, [Cl$^-$]$_{free}$, the free cation, [S^+]$_{free}$, and the mean ionic molarity of the surfactant, i.e., ([Cl$^-$]$_{free}$x[S^+]$_{free}$)$^{0.5}$, on [C$_{14}A$Me$_3$Cl], at 25 °C

We now discuss

1. The rationale for favorable ΔG^0_{ads} and ΔG^0_{mic} of the title surfactants, relative to R'Me$_3$Cl.
2. Further evidence (IR) for localization of the micellar interface close to the amide nitrogen.
3. Effects of substitution of one of the trimethylammonium groups of RAMe$_3$Cl by a benzyl group.

Application of Eqs. (1) and (2) shows that the reason for 1 is the larger contribution of the head group to the appropriate Gibbs free energy. Our FTIR results indicate that this is due to intermolecular hydrogen bonding of surfactant molecules, via the amide group, akin to that of amides, polypeptides, and other surfactants that carry the –CONH head group [8, 9, 10, 11, 12]. N-Methylacetamide has been extensively employed to model hydrogen-bonding interactions in proteins, so a discussion of the frequency of its amide I band is relevant. In dilute aqueous solution, N-methylacetamide is completely hydrated, its $\nu_{C=O}$ is around 1626 cm^{-1} [26, 27, 28]. Solubilization of the amide in binary mixtures whose polarity mimics that of interfacial water, for example, aqueous acetonitrile and aqueous dimethyl sufoxide [5], results in an increase of $\nu_{C=O}$, directly proportional to the concentration of the organic component of the binary mixture. This has been attributed to decreased hydration of the CO group, i.e., substitution of some of the CO–water hydrogen bonds by NH–CO bonds [23, 26]. Finally, $\nu_{C=O}$ in pure organic solvents is much higher than that of hydrogen-bonded amide, for example, hexane

1697 cm^{-1}, tetrahydrofuran 1683 cm^{-1}, and dimethyl sufoxide 1,667 cm^{-1} [26].

As Fig. 2b shows, at a $C_{10}A$Me$_3$Cl concentration below the cmc, $\nu_{C=O}$ is constant at 1626 cm^{-1}, indicating that the amide group of the monomer is exposed to water, i.e., the CO group is strongly hydrated [11, 23, 26, 27]. There is a break at the cmc, after which $\nu_{C=O}$ increases, then levels off at 1632 cm^{-1}, at around 0.15 mol L^{-1}. Micellization is akin to transfer of the head group from bulk water to (less polar) interfacial water [5]. This explains the first break at the cmc, and the increase of $\nu_{C=O}$, some of the –CO–water hydrogen bonding is replaced hydrogen bonding between the surfactant amide groups. This process apparently continues until the second break at 1632 cm^{-1}. Whether the latter indicates a second cmc, attributed to a change of micellar geometry, is outside the scope of the present work, and will be the subject of a future study.

The strength of the previously mentioned hydrogen bonding is further corroborated by the following

1. We studied the dependence of $\nu_{C=O}$ of sodium 2-decanoyloxyethane sulfonate on its concentration, below and above the cmc (0.023 mol L^{-1}, determined by conductance, in agreement with 0.011 mol L^{-1}, 30 °C, surface tension [29]). The carbonyl frequency was found to be constant within the resolution limit employed (± 1 cm^{-1}).
2. $\Delta\nu$ (= $\nu_{C=O}$ after the cmc− $\nu_{C=O}$ before the cmc) is 6 and less than 3 cm^{-1} for RAMe$_3$Cl and sodium decanoate, respectively [21].

Point 1 shows that there is negligible change in hydration of interfacial –C = O, when the surfactant carries no amide head group. Point 2 shows that $\Delta\nu$ for RAMe$_3$Cl is larger, although the soap carries the strongly hydrated, solvent-polarity-sensitive carboxylate anion. In summary, hydrogen bonding between molecules of RAMe$_3$Cl at the solution/air interface and/or in the aggregate is appreciable; this is responsible for the lower, i.e., more favorable free energies of adsorption and/or micellization of RAMe$_3$Cl, relative to RMe$_3$Cl. The fact that the final $\nu_{C=O}$ of $C_{10}A$Me$_3$Cl is much lower than that of $\nu_{C=O}$ of N-methylacetamide in nonpolar or dipolar aprotic solvents (vide supra) corroborates our argument that the surfactant amide group is not localized in (nonpolar) micellar interior, see point 2 earlier.

Relative to RAMe$_3$Cl, the corresponding RABzMe$_2$Cl shows more favorable Gibbs free energies of adsorption and micellization; larger A_{min}, and smaller cmc, α_{mic}, and N_{agg} (see point 3 earlier and Table 2). These results can be readily explained on the basis of differences between the benzyl and the methyl group. For simplicity, we take trimethylamine and benzyldimethylamine as models for head groups of RAMe$_3$Cl, and the corresponding RABzMe$_2$Cl, respectively, and we compare two properties, the volume, and $\log P_{oct}$. The latter refers to the partition coefficient between n-octanol and water, i.e., log([substance]$_{octanol}$/[substance]$_{water}$). It is a quantitative measure of the hydrophilic/ hydrophobic character of a molecule, or a segment therefrom [30]. The volumes are 0.095 and 0.182 nm^3, and $\log P_{oct}$ is 0.16 and 1.98, for trimethylamine, and benzyldimethylamine, respectively. Therefore, the benzyl group is more voluminous and more hydrophobic than the methyl group. It is known that the minimum area per surfactant molecule at the solution/air interface increases as a function of increasing the size of the head group. This entails a decrease in N_{agg} and an increase in α_{mic}, since the micelle becomes more loosely packed [1, 2, 3], in agreement with our data for the two surfactant series. On the other hand, the contribution of $(\Delta G^0_{\text{head group}} + \Delta G^0_{CH_3})$ to the Gibbs free energies of adsorption and/or micellization is sizeable; therefore an increase in head group hydrophobicity should result in more favorable Gibbs free energies, again in agreement with our results. Finally, Table 2 also shows the quantity cmc/C_{20}, a measure of the relative effects of structural changes on surfactant micellization and adsorption [2]. As shown in Table 2, the order is R'Me$_3$Cl$\gg$$RA$BzMe$_2$Cl > RAMe$_3$Cl. That is, the segment –CONH(CH$_2$)$_2$– of the head group seems to favor micellization more than adsorption of RAMe$_3$Cl, relative to R'Me$_3$Cl. For amide-containing surfactants, the methyl group favors micellization more than adsorption.

Conclusions

A homologous series of 2-(acylaminoethyl)trimethylammonium chloride surfactants have been synthesized and their adsorption at the solution/air interface and aggregation in aqueous solution were studied by conductivity, surface tension, EMF (in H_2O), and FTIR (in D_2O) measurements. Gibbs free energies of adsorption and/or of micellization were separated into contributions from discrete surfactant segments. Both types of free energies are lower for RAMe$_3$Cl than those of corresponding R'Me$_3$Cl, owing to hydrogen bonding between the surfactant amide group. Differences between physicochemical properties of solutions of RAMe$_3$Cl and RABzMe$_2$Cl are attributed to differences between the volume and the hydrophobicity of the methyl and benzyl groups.

Acknowledgements We thank the FAPESP for financial support and for a predoctoral fellowship to S.S., the CNPq for a research productivity fellowship to O.A.ES, Paulo A.R. Pires for his help with calculations, and H. Chaimovich and I.M. Cuccovia for making the chloride-ion-selective electrode available to us.

Appendix

$A_{\min}$ and ΔG^0_{ads} from surface tension data

We employed the following equation to calculate $A_{\min}$ [2]:

$$A_{\min} = \frac{10^{18}}{N_{\text{Av}}\Gamma_{\max}}, \tag{3}$$

where $\Gamma_{\max}$ and N_{Av} refer to the maximum surface excess concentration of surfactant and Avogrado's number, respectively. $\Gamma_{\max}$ was calculated from the Gibbs adsorption isotherm:

$$\Gamma_{\max} = \frac{1}{4.606RT}\left(\frac{\partial\pi}{\partial\left(\log[\text{Surf}]_{\text{t}} + \log f_{\pm}\right)}\right), \tag{4}$$

where $[\text{Surf}]_{\text{t}}$, $f_{\pm}$, and π refer to total surfactant concentration, the mean activity coefficient of surfactant cation and counterion in the aqueous phase, and surface pressure ($\pi = \gamma_{\text{H}_2\text{O}} - \gamma_{\text{solution}}$), respectively.

On the mol fraction scale, ΔG^0_{ads} (joules per mole) is calculated from Eq. (5) [2, 15]:

$$\Delta G^0_{\text{ads}} = 5705.8(\log\chi_{20} + \log f_{\pm}) - (6.023 \times 20 \times A_{\min}), \tag{5}$$

where χ_{20} is to the surfactant mole fraction required to reduce $\gamma_{\text{H}_2\text{O}}$ by 20 mN m^{-1}, and $A_{\min}$ is in angstroms squared.

cmc, α_{mic}, and thermodynamic parameters of micellization

Critical micelle concentration

As Figs. 1 and 2a show, plots of the solution properties versus $[\text{Surf}]_{\text{t}}$ gave two straight lines intersecting at the cmc. The FTIR plot, Fig. 2b, showed two breaks; the first corresponds to the cmc.

α_{mic}

α_{mic} was obtained by three procedures, the first two rely on conductance, whereas the third employs EMF. According to Frahm et al., α_{mic} is given by [17]

$$\alpha_{\text{mic}} = (S_2/S_1), \tag{6}$$

where S_2 and S_1 refer to slopes of the conductance plot above and below the cmc, respectively. The following equation is that of Evans [18]:

$$1000S_2 = \frac{\alpha^2_{\text{mic}}}{N_{\text{agg}}^{-2/3}}(1000S_1 - \Lambda_{\text{Cl}^-}) + \alpha_{\text{mic}}\Lambda_{\text{Cl}^-}, \tag{7}$$

where Λ_{Cl^-} refers to the equivalent conductance of the surfactant counterion at infinite dilution. Calculation of α_{mic} from EMF measurement was carried out as follows [20]. The dependence of solution EMF (ΔE_{obs} in millivolts) on $[\text{Surf}]_{\text{t}}$ is given by

$$\Delta E_{\text{obs}} = \Delta E^0 - (2.303RT/F)\log[\text{Surf}]_{\text{t}}, \tag{8}$$

where ΔE^0 and F refer to the EMF of the reference state ($[\text{Surf}]_{\text{t}} = 1.0$ mol L^{-1}) and the Faraday constant, respectively. The plot of ΔE_{obs} versus $\log[\text{Surf}]_{\text{t}}$, over a wide range of concentration (about 0.1cmc–60cmc), shows two linear parts, before and after the cmc, as shown in Fig. 4. The intercepts of these parts, ΔE^0 and $\Delta E'^0$, respectively, are related to the cmc by

$$\Delta E'^0 - \Delta E^0 = (2.303RT/\text{F})\log\alpha_{\text{mic}}, \tag{9}$$

from which α_{mic} can be calculated.

N_{agg}

Calculation of N_{agg} was based on the assumption of spherical aggregates and a stretched, all-trans monomer conformation inside the micelle (Spartan-Pro program package, version 5.1, Wave Function, Irvine, CA). The micellar N_{agg} calculated for both possibilities of the interface (amide nitrogen and/or quaternary ammonium ion, $\text{RCONH(CH}_2)_2\text{N}^+(\text{CH}_3)_3\text{Cl}^-$) were 43, 61, 82, 107 (amide nitrogen) and/or 72, 96, 122, 152 (quaternary ammonium ion), for $R\text{CO} = \text{C}_{10}$, C_{12}, C_{14}, and C_{16}, respectively. The same program was used to calculate the volumes of trimethylamine and benzyldimethylamine, respectively.

EMF results were also employed to calculate N_{agg}, as follows [25]. The dependence of $[\text{Cl}^-]_{\text{free}}$ on $[\text{Surf}]_{\text{t}}$, and the concentration of free surfactant cation, $[S^+]_{\text{free}}$, is given by

$$[\text{Cl}^-]_{\text{free}} = \left(1 - N_{\text{ci}}/N_{\text{agg}}\right)[\text{Surf}]_{\text{t}} + \left(1 - N_{\text{ci}}/N_{\text{agg}}\right)[S^+]_{\text{free}}, \tag{10}$$

were N_{ci} is the number of counterions associated with the micelle. N_{agg} can be calculated from (experimental) $[\text{Cl}^-]_{\text{free}}$ and $[\text{Surf}]_{\text{t}}$, by Eq. (10), provided that N_{ci} and $[S^+]_{\text{free}}$ are available. These were obtained as follows: the mass-action law for micelle formation was assumed to hold; α_{mic} and cmc, obtained from EMF measurement, were employed; best values for N_{ci} and $[S^+]_{\text{free}}$ were obtained by iteration, by using the following equations:

$$N_{\text{ci}} = N_{\text{agg}} - (\alpha_{\text{mic}}N_{\text{agg}}), \tag{11}$$

$$[S^+]_{\text{free}} = [\text{Surf}]_{\text{t}} - N_{\text{agg}}[\text{micelle}], \tag{12}$$

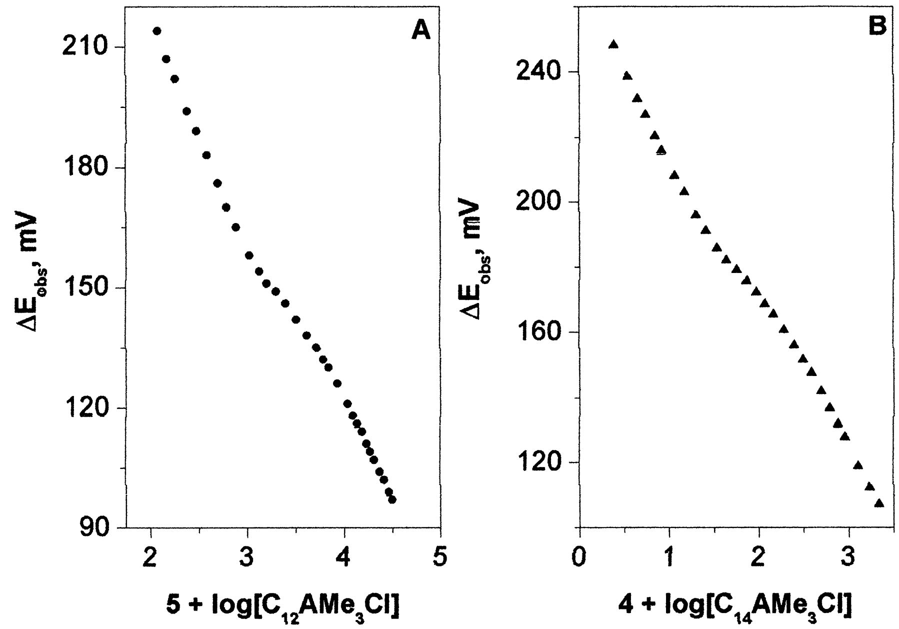

Fig. 4. Dependence of solution electromotive force, measured with a chloride-ion electrode on log[surfactant], for $C_{12}AMe_3Cl$ and $C_{14}AMe_3Cl$, respectively

where [micelle] is the concentration of micelles calculated from the mass-action model by

$$[\text{micelle}] = K[S^+]_{\text{free}}^{N_{\text{agg}}}[\text{Cl}^-]_{\text{free}}^{N_{\text{ci}}}, \tag{13}$$

where K is the equilibrium constant of micelle formation, calculated from the cmc, N_{ci}, and N_{agg} by [31]

$$1/K = 2N_{\text{agg}}\left(N_{\text{agg}} + N_{\text{ci}}\right)\text{cmc}^{\left(N_{\text{agg}}+N_{\text{ci}}\right)}. \tag{14}$$

A BASIC script that relies on the S-Plus 2000 program package (MathSoft, Seattle, USA) was written and employed to calculate N_{agg}. A typical example for $[\text{Cl}^-]_{\text{free}}$ versus $[\text{Surf}]_t$, calculated by iteration, is shown in Fig. 3. The uncertainty in N_{agg} is ±10%.

Free energy of micellization

The free energy of micellization was calculated from [2]

$$\Delta G^0_{\text{mic}} = (2 - \alpha_{\text{mic}})RT\ln\chi_{\text{cmc}}, \tag{15}$$

where $\chi_{\text{cmc.}}$ is the cmc expressed on the mole fraction scale, and α_{mic} is that calculated by the method of Frahm or Evans.

References

1. Hiemenz PC, Rajagopalan R (1997) Principles of colloid and surface chemistry. Dekker, New York, pp 297, 355
2. Rosen MJ (1989) Surfactants and interfacial phenomena. Wiley, New York, pp 33, 108
3. (a) Kahlweit M, Strey R, Haase D, Firman P (1988) Langmuir 4785; (b) Evans DF, Wennerström H (1994) The colloidal domain. VCH, New York, pp 451
4. Bazito RC, El Seoud OA, Barlow GK, Halstead TK (1997) Ber Bunsenges Phys Chem 101:1933
5. Tada EB, Novaki LP, El Seoud OA (2001) Langmuir 17:652
6. (a) Lacko I, Mlynarcik D, Jadronova M, Karoskova J (1987) CS 237747, Chem Abstr 108:186165; (b) Devinky F, Masarova L, Lacko I (1987) CS 240390, Chem Abstr 108:221286; (c) Login RB, Chaudhuri RK, Tracy DJ, Helioff MW (1989) US 4837013A, Chem Abstr 111:201398; (d) Oshima T (1989) JP 01006210, Chem Abstr 111:20620; (e) Oshima T (1990) JP 02160714, Chem Abstr 113:217792; (f) Iwai H, Nomura T, Shiraiwa T, Mori S, DaihoY (1996) JP 08206581, Chem Abstr 125:250488; (g) Kaneda E, Ohtaki H, Oka S (1994) JP 54043731, Chem Abstr 91:99908; (h) Bailey AV et al (1974) US 473477, Chem Abstr 84:79590
7. (a) Mod RR, Magne FC, Skau EL, Sumrell GJ (1971) Med Chem 14:558; (b) Bailey AV, Sumrell G, Gurtner TE (1974) J Am Oil Chem Soc 51:515
8. (a) Bazito RC, El Seoud OA (2001) Carbohyd Res 323:95; (b) Bazito RC, El Seoud OA (2001) J Surfactant Deterg 4:395; (c) Bazito RC, El Seoud OA (2002) Langmuir 18:4362
9. Shimizu S, El Seoud OA (2003) Langmuir 19:238
10. (a) Kollman P (1993) Chem Rev 93:2395; (b) Ludwig RO, Winter R, Weinhold F, Farrar TC (1998) J Phys Chem B 102:9312
11. Huelsekopf M, Ludwig R (2001) Mag Res Chem 39:127

12. (a) Solans C, Infante R, Azemar N, Wärnheim T (1989) Prog Colloid Polym Sci 79:70; (b) Kunieda H, Nakamura K, Infante R, Solans C (1992) Adv Mater 4:291
13. Eastoe J, Nave S, Downer A, Paul A, Rankin A, Tribe K (2000) Langmuir 16:4511
14. Tanford C (1991) The hydrophobic effect: formation of micelles and biological membranes. Krieger, FL
15. Rosen MJ, Li F (2002) Environ Sci Technol 35:954
16. Blois DW, Swarbrick J (1971) J Colloid Interface Sci 36:227
17. Frahm J, Diekmann S, Haase A (1980) Ber Bunsenges Phys Chem 84:566
18. Evans HC (1956) J Chem Soc 579
19. Evans DF, Allen M, Ninham BW and Fouda A (1984) J Sol Chem 13:87
20. Gaillon L, Hamidi M, Lelièvre J, Gaboriaud R (1997) J Chim Phys 94:707
21. Umemura J, Mantsch HH, Cameron DG (1981) J Colloid Interface Sci 83:558
22. Yang PW, Mantsch HH (1986) J Colloid Interface Sci 113:218; (c) Etori F, Yamada H, Taga Y, Okabayashi K, Ohshima HK, O'Connor CJ (1997) Vib Spectrosc 14:133
23. (a) Lafrance D, Marion D, Pézolet (1990) M Biochem 29:4592
24. (a) Nilsson A, Holmgren A, Lindblom G (1994) Chem Phys Lipids 69:219; (b) Domingo JC, Mora M, de Madariaga MA (1994) Chem Phys Lipids 69:229; (c) Domingo JC, de Madariaga MA Chem Phys Lipids 84:147
25. (a) Sasaki T, Hattori M, Sasaki J, Nukina K (1975) Bull Chem Soc Jpn 48:1397; (b) Moroi Y (1988) J Colloid Interface Sci 122:308.
26. Eaton G, Symons MCR, Rastogi PP (1989) J Chem Soc Farday Trans 1 85:3257
27. Miyazawa T, Shimanouchi T, Mizushima S (1958) J Chem Phys 29:611
28. (a) Chen CYS, Swenson CA (1969) J Phys Chem 73:2999; (b) Symons MCR (1993) J Mol Struct 297:133; (c) Schweitzer-Stenner R, Sieler G, Mirkin NG, Krimm S (1998) J Phys Chem A 102:118
29. Hioka T, Morohara K, Meguro K (1970) Bull Chem Soc Jpn 43:3913
30. Leo A (1993) J Chem Rev 93:1281
31. Shah SS, Jamroz NV, Sharif Q M (2001) Colloids Surf A 178:199